Multiple Origins and Genomic Basis of Complex Traits in Sighthounds

Wu-Lue Li,[†,1,2] Yan-Hu Liu,[†,1] Jin-Xiu Li,[†,1] Meng-Ting Ding,[†,1,2] Adeniyi C. Adeola,[1,3] Jainagul Isakova,[4] Almaz A. Aldashev,[‡,4] Min-Sheng Peng,[1,3,5] Xuezhen Huang,[5] Guoli Xie,[1] Xi Chen,[6,7] Wei-Kang Yang,[7] Wei-Wei Zhou,[1] Zeinab Amiri Ghanatsaman,[8] Sunday C. Olaogun,[9] Oscar J. Sanke,[10] Philip M. Dawuda,[11] Marjo K. Hytönen,[12,13,14] Hannes Lohi,[12,13,14] Ali Esmailizadeh [iD],[*,1,15] Andrey D. Poyarkov,[*,16] Peter Savolainen,[*,17] Guo-Dong Wang,[*,1,3] and Ya-Ping Zhang [iD][*,1,2,3,5]

[1]State Key Laboratory of Genetic Resources and Evolution, Yunnan Laboratory of Molecular Biology of Domestic Animals, Kunming Institute of Zoology, Chinese Academy of Sciences, Kunming, China

[2]Kunming College of Life Science, University of Chinese Academy of Sciences, Kunming, China

[3]Sino-Africa Joint Research Center, Chinese Academy of Sciences, Kunming, China

[4]Laboratory of Molecular and Cell Biology, Institute of Molecular Biology and Medicine, Bishkek, Kyrgyzstan

[5]State Key Laboratory for Conservation and Utilization of Bio-Resources in Yunnan, School of Life Sciences, Yunnan University, Kunming, China

[6]Research Center for Ecology and Environment of Central Asia, Chinese Academy of Sciences, Urumqi, China

[7]Key Laboratory of Biogeography and Bioresource in Arid Land, Xinjiang Institute of Ecology and Geography, Chinese Academy of Sciences, Urumqi, China

[8]Animal Science Research Department, Fars Agricultural and Natural Resources research and Education Center, Agricultural Research, Education and Extension Organization (AREEO), Shiraz, Iran

[9]Department of Veterinary Medicine, Faculty of Veterinary Medicine, University of Ibadan, Ibadan, Nigeria

[10]Ministry of Agriculture and Natural Resources, Taraba State Government, Jalingo, Nigeria

[11]Department of Animal Science, Faculty of Agriculture, National University of Lesotho, Roma, Southern Africa

[12]Department of Medical and Clinical Genetics, University of Helsinki, Helsinki, Finland

[13]Folkhälsan Research Center, Helsinki, Finland

[14]Department of Veterinary Biosciences, University of Helsinki, Helsinki, Finland

[15]Department of Animal Science, Faculty of Agriculture, Shahid Bahonar University of Kerman, Kerman, Iran

[16]Severtsov Institute of Ecology and Evolution, Russian Academy of Science, Moscow, Russia

[17]KTH Royal Institute of Technology, School of Engineering Sciences in Chemistry, Biotechnology and Health, Department of Gene Technology, Science for Life Laboratory, Solna, Sweden

[†]These authors contributed equally to this work.

[‡]Passed away

*Corresponding authors: E-mails: zhangyp@mail.kiz.ac.cn; wanggd@mail.kiz.ac.cn; savo@kth.se; poyarkov@yandex.ru; aliesmaili@uk.ac.ir.

Associate editor: Daniel Falush

Abstract

Sighthounds, a distinctive group of hounds comprising numerous breeds, have their origins rooted in ancient artificial selection of dogs. In this study, we performed genome sequencing for 123 sighthounds, including one breed from Africa, six breeds from Europe, two breeds from Russia, and four breeds and 12 village dogs from the Middle East. We gathered public genome data of five sighthounds and 98 other dogs as well as 31 gray wolves to pinpoint the origin and genes influencing the morphology of the sighthound genome. Population genomic analysis suggested that sighthounds originated from native dogs independently and were comprehensively admixed among breeds, supporting the multiple origins hypothesis of sighthounds. An additional 67 published ancient wolf genomes were added for gene flow detection. Results showed dramatic admixture of ancient wolves in African sighthounds, even more than with modern wolves. Whole-genome scan analysis identified 17 positively selected genes (PSGs) in the African population, 27 PSGs in the European population, and 54 PSGs in the Middle Eastern population. None of the PSGs overlapped in the three populations. Pooled PSGs of the three populations were significantly enriched in "regulation of release of sequestered calcium ion into cytosol" (gene ontology: 0051279), which is related to blood

Open Access

circulation and heart contraction. In addition, *ESR1*, *JAK2*, *ADRB1*, *PRKCE*, and *CAMK2D* were under positive selection in all three selected groups. This suggests that different PSGs in the same pathway contributed to the similar phenotype of sighthounds. We identified an *ESR1* mutation (chr1: g.42,177,149 T > C) in the transcription factor (TF) binding site of Stat5a and a *JAK2* mutation (chr1: g.93,277,007 T > A) in the TF binding site of Sox5. Functional experiments confirmed that the *ESR1* and *JAK2* mutation reduced their expression. Our results provide new insights into the domestication history and genomic basis of sighthounds.

Key words: sighthounds, origin, artificial selection, population genomics.

Introduction

Human–dog coexistence can be traced back approximately 14,000–32,000 years (Savolainen et al. 2002; Ding et al. 2012; Thalmann et al. 2013; Frantz et al. 2016; Wang et al. 2016). At present, over 400 breeds are registered with American Kennel Club (AKC) and Fédération Cynologique Internationale (FCI). Due to their extensive phenotypic diversity, dogs serve as valuable subjects for comparative genomics research (Zhou et al. 2022). Notably, various genome-wide association studies (GWAS) have elucidated the genetic basis of phenotype variations in dogs, such as body size, coat color, limb length, skull shape, and longevity (Schmutz et al. 2002; Sutter and Ostrander 2004; Rimbault et al. 2013; Plassais et al. 2019). Furthermore, investigations on positive selection have shed light on the evolutionary processes underlying certain dog breeds selectively bred by humans for specific purposes like sport-hunting dogs (Kim et al. 2018).

The majority of modern dog breeds emerged through deliberate reproductive isolation and artificial selection practices during the mid-19th century (Parker et al. 2004) contributed to the majority of modern breeds. However, certain sighthound breeds can trace their origins back to the hunting demand of prehistoric humans. Previous research has indicated that Greyhounds lack the main haplotype found in all dogs, supporting their ancient lineage and implying that they represent a well-preserved primal sighthound breed (Savolainen et al. 2002). Supporting this perspective, Greyhounds boast a pedigree history dating back approximately 8,000 years (Como 2004). Furthermore, analysis of molecular markers further identified Afghan hounds and Salukis as two of the most ancient breeds (Parker et al. 2004). These findings imply that sighthounds may have played an important role in the transition from a hunter-gathering to an agrarian society in ancient human civilizations, potentially initiating the early formation of distinct breeds (Parker et al. 2017). Due to their ancient lineages and absence of written records, the precise origin of sighthound breeds remains ambiguous. Legends and accounts of sighthounds can be found across Africa, Asia, the Mediterranean coast, and other regions, supported by intriguing archeological evidence (supplementary fig. S1, Supplementary Material online). Following the migration of human populations, these breeds dispersed to various parts of the world, including the Americas and Australia, gaining widespread recognition.

Sighthounds exhibit a wide range of characteristics. For instance, the Irish Wolfhound is exceptionally tall, with males reaching a minimum height of 32 inches (approximately 81 cm) at the shoulder, while the Italian Greyhound only has an average height of 33–38 cm. Sighthound breeds also display considerable coat variation, such as the Afghan Hound, possessing thick and long hair suitable for cold mountainous areas, and others such as the Azawakh, possessing shorthair and lacking the undercoat layer. However, while sighthound breeds encompass a broad spectrum, they do share distinctive phenotypes including a deep chest, slim limbs, and lean body (Dutrow et al. 2022), as well as specialized hematological features (Court 1999). These physical traits are associated with the unique specialization of sighthounds, which involves the visual detection of prey, followed by their pursuit and capture with exceptional speed. To facilitate their swift running abilities, their deep yet narrow chests provide increased pleural volume, accommodating the placement of lungs and heart without a significant increase in body cross-section (Hancock 2012). These distinctive features reflect the extensive artificial selection that has shaped sighthound breeds, ensuring that their agility and focus on hunting, with the selection for keen eyesight, further reflected in their elongated and narrow skulls (McGreevy et al. 2013). The profound impact of artificial selection extends beyond physical traits to the neural and cardiovascular systems of these dogs. For example, Greyhounds frequently suffer from hyperthermia and hyperhomocysteinemia (Brunson and Hogan 2004; Kent et al. 2014; Pols et al. 2016; Heilmann et al. 2017), and sighthound arterial pressure is the highest among domestic dogs (Bodey and Michell 1996).

To further investigate the distinctive characteristics of sighthounds, we conducted genome sequencing of 123 genomes of sighthounds from Africa, Europe, Russia, and the Middle East, as well as 12 genomes of village dogs from the Middle East. By integrating these data with publicly available genomes of five sighthounds, 98 other dogs, and 31 gray wolves, we reconstructed the population structure and demographic history of the sighthounds and further explored the origin of and gene flow across different breeds of sighthounds from a genomic perspective. Furthermore, based on the identification of signatures of positive selection, we examined the potential genomic basis responsible for the shared phenotypic traits observed in sighthounds.

Results

Geographic Distribution of Sighthounds

In the present study, we collected samples from 123 sighthounds from 13 countries in Eurasia and Africa, as well as

12 village dogs from Iran (supplementary table S1, Supplementary Material online). Furthermore, we incorporated publicly available genome data from various sources, including five sighthounds, 48 village dogs, 50 pedigree breeds, and 31 gray wolves (supplementary table S2, Supplementary Material online) (Freedman et al. 2014; Gou et al. 2014; Fan et al. 2016; Marsden et al. 2016; Wang et al. 2016). The representative, sighthound breeds included six European breeds (five Greyhounds, three Irish Wolfhounds, three Scottish Deerhounds, one Galgo, one Italian Greyhound, and two Hungarian Greyhounds [Magyar Agár]), two Russian breeds (23 Borzois and 13 Chortais); two Middle Eastern breeds (four Afghan Hounds and three Tazys from Iran); and two Central Asian breeds from (15 Taigans from Kyrgyzstan and 19 Tazys from Kazakhstan and Turkmenistan), as well as 15 African native sighthounds from Nigeria (supplementary fig. S2, Supplementary Material online) and seven Shaanxi sighthounds from China (fig. 1a). The Shaanxi sighthound, also known as the Xi dog, is a native Chinese sighthound breed characterized by a linkage disequilibrium (LD) decay distance compared with European breeds (Yang et al. 2019). Overall, our data set covered a wide range of sighthound origins, encompassing most possible lineages.

Whole-Genome Sequencing and SNP Calling

Whole-genome sequencing was conducted for 135 individuals, with performed to an average coverage of 12.84× (ranging from 4.61 to 25.75) and 134 published individuals, with an average coverage of 15.90× (ranging from 7.00 to 35.07) (supplementary tables S1 and S2, Supplementary Material online). Following stringent quality filtering (see Materials and Methods), we retained 26.54 million single nucleotide polymorphisms (SNPs) and 6.24 million small indels on the autosomes for further analysis. The sex chromosomes were excluded due to their hemizygote state in male, which makes them more susceptible to demographic and selective effects than autosomes (Gottipati et al. 2011; Meisel and Connallon 2013).

Population Structure, Phylogeny, and Genetic Diversity

Principal component analysis (PCA) was conducted to investigate the relationships between individuals. The results visualized two-dimensionally demonstrated that the dogs formed a distinct and tight cluster, separate from wolves (supplementary fig. S3a, Supplementary Material online). When focusing on the dogs, we observed a division between East Asian indigenous dogs and other dog populations. Interestingly, Shaanxi sighthounds clustered tightly with European sighthounds rather than with indigenous Chinese dogs (fig. 1b and supplementary fig. S3b, Supplementary Material online). Consequently, we conducted further PCA solely on dogs, excluding the lineage of East Asian indigenous dogs, which revealed a clear geographic pattern (fig. 1b): 1) African native sighthounds

clustered with African village dogs, representing sister branch of Middle Eastern dogs; 2) Middle Eastern sighthounds clustered with Middle Eastern village dogs; 3) European sighthounds clustered with breeds from Europe; and 4) Russian sighthounds split into two clusters, with the Chortai breed showing closer proximity to European dogs than to Borzoi dogs. To further explore the genetic relationships among these individuals, we performed structure analysis to cluster individuals into different groups (fig. 1b). The results aligned with the PCA findings. The East Asian dogs separated initially, followed by the formation of four distinct geographically based clusters: Europe, Middle East, Africa, and Russia. Notably, the Chortai breed was found to be an admixture of Borzoi and Middle Eastern dogs.

Further, phylogenetic analysis showed that dogs diverged from wolves at the root of the tree. Middle Eastern and African dogs formed sister branches, while the African native sighthounds exhibited a unique pattern, occupying positions closer to the wolves than the branches of African village dog. Notably, as African dogs have been established as a distinct population based on mitochondrial DNA and nuclear genomes (Boyko et al. 2009; Wang et al. 2016; Adeola et al. 2017; Liu et al. 2018), the African native sighthounds may represent a subbreed with an unknown lineage. European dogs grouped together with Russian dogs. Furthermore, the sighthounds exhibited a distinct separation from other dog breeds and displayed a clear geographic pattern, reflecting their breeding history. The Borzoi and Chortai breeds also formed a separate lineage, closely clustering with other European breeds.

After grouping analysis, genetic diversity (θ_π) within our data set was calculated (supplementary fig. S4, Supplementary Material online). Results showed that all sighthounds exhibited lower diversity than their corresponding indigenous dogs ($P < 6.86 \times 10^{-8}$) for all three comparisons. Notably, European sighthounds hold the lowest diversity (1.07×10^{-3} average), while Eastern Asian village dogs showed the highest diversity (1.31×10^{-3} average). Both Middle Eastern village dogs and sighthounds demonstrated relatively high diversity.

Furthermore, our study identified five types of native sighthounds not officially recognized by FCI or AKC: African native sighthound, Chortai, Shaanxi sighthound, Taigan, and Tazy. To identify possible differences between native sighthounds and other recognized sighthounds, we analyzed their genetic diversity, inbreeding coefficient, and runs of homozygosity (ROH). Compared with recognized sighthounds, most native sighthounds displayed significantly higher diversity, lower inbreeding coefficient, and shorter ROH (supplementary fig. S5, Supplementary Material online).

Demographic History and Gene Flow

The phylogeny of sighthounds could be due to admixture between breeds and native dogs. To investigate the
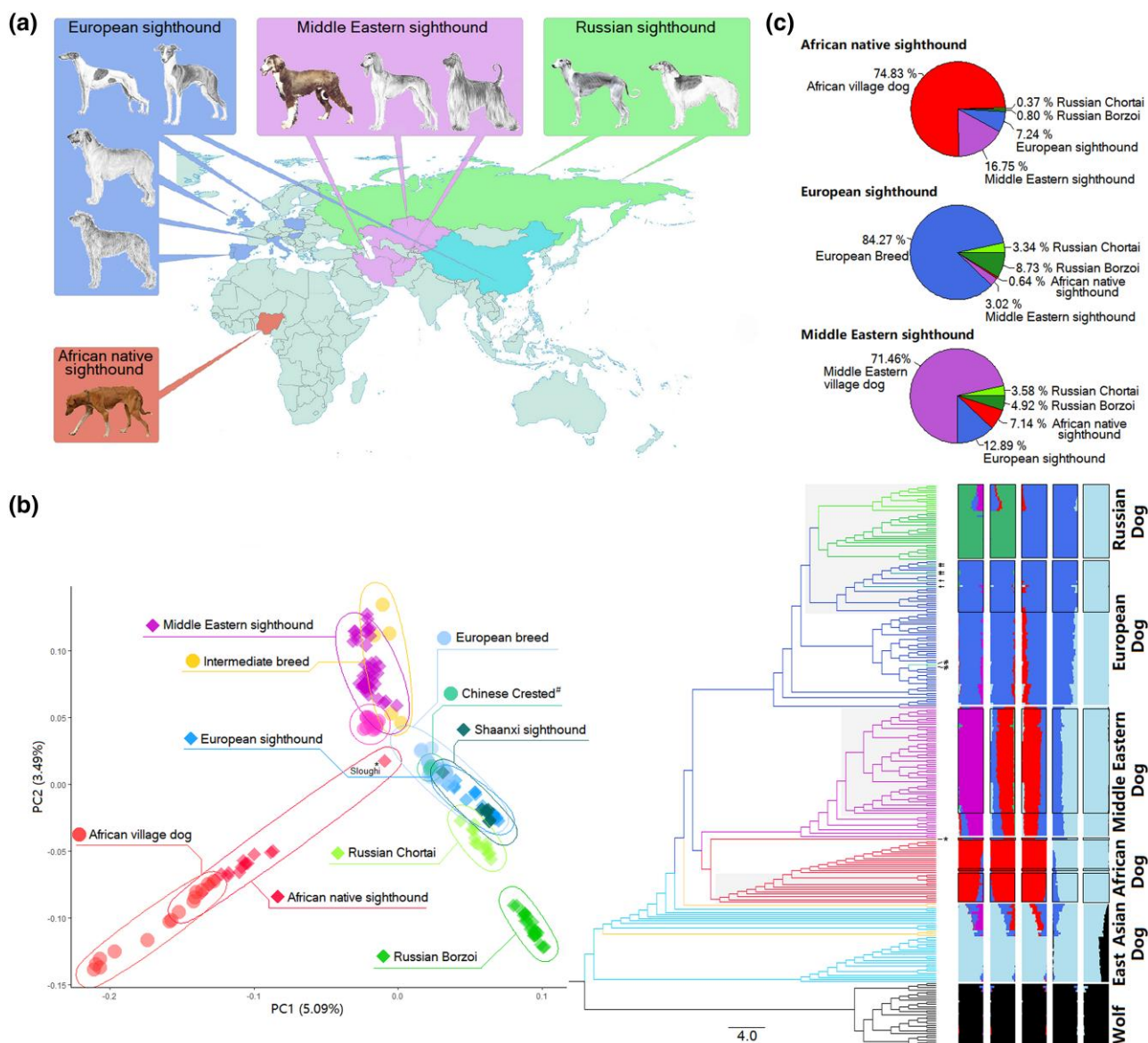
Fig. 1. Geographic and genetic grouping of samples. (*a*) Locations of sample collection, with photos of dogs sourced from AKC and Wiki. (*b*) PCA plot showing the distribution of all dogs, excluding East Asian village dogs (left); neighbor-joining phylogenetic tree highlighting relationships between samples (middle); and admixture analysis displaying population structure (right). Sighthound individuals are represented by shaded branches in the phylogenetic tree, while the framed structure bar indicates sighthound individuals. Notably, sighthound samples from the Middle East, Africa, and Europe closely aligned with their respective local samples. Shaanxi sighthounds (indicated by arrowhead pointing to clades) merged with the European sighthound population in both the phylogenetic tree and admixture analysis. The Sloughi individual (marked by asterisks) was excluded from selection and population analysis due to genetic admixture and its outlier position in PCA, neighbor-joining tree, and structure analysis. (*c*) RFMix result illustrating genetic ancestry of sighthound populations.

presence of migration events and their impact on phylogeny, we performed TreeMix analysis (supplementary fig. S6, Supplementary Material online). The results corroborated the patterns observed following analysis of PCA, structure, and phylogeny (fig. 1*b*). Gene flows between African dogs and modern wolves were identified (supplementary fig. S6, Supplementary Material online). To validate the gene flow detected by TreeMix, we used the R package admixr to further analyze *D*-statistics for all sighthounds and modern wolves (Petr et al. 2019). The analysis revealed that gene flow was not widespread

across all sighthounds but rather primarily observed in Shaanxi sighthounds, African native sighthounds, and Taigan (|*Z*| > 3.00) (fig. 2*b*).

As gray wolves are not naturally found in Africa (Rueness et al. 2011; Koepfli et al. 2015; Viranta et al. 2017; Gopalakrishnan et al. 2018), it is plausible that African native sighthounds have retained some genetic components from ancient wolves. To investigate this possibility, we obtained whole-genome data from 67 published ancient wolves from Europe, Siberia, and northwestern North America (Bergstrom et al. 2022).
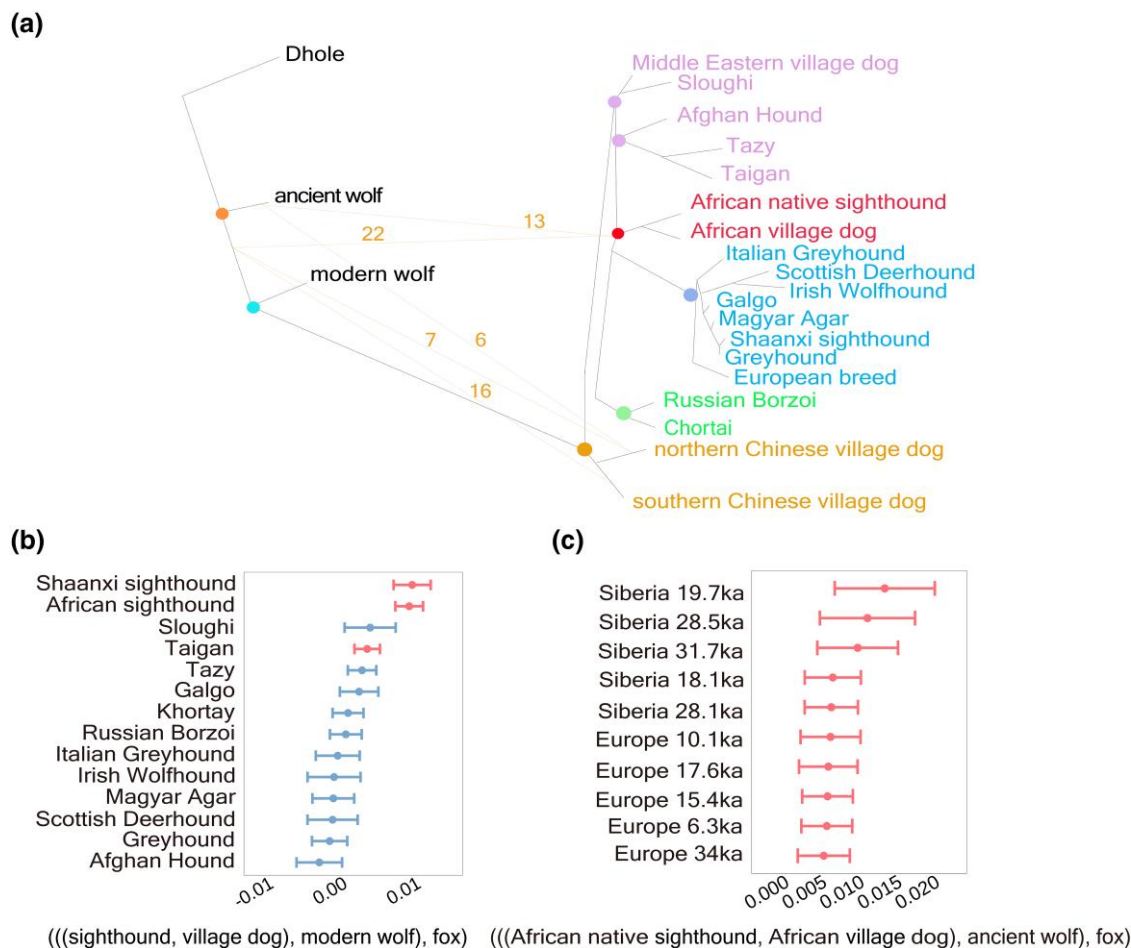
Fig. 2. Gene flow between sighthounds and ancient wolves. (*a*) TreeMix simulation diagram showing gene flow between sighthounds and each ancient wolf. Lines with arrows indicate gene flow and direction, and numbers on the lines represent the frequency of these events in the TreeMix analysis between the 67 ancient wolves and sighthounds. (*b*) Outgroup *D*-statistics depicting phylogeny analysis; red bars indicate significant differences from nonadmixed part of sighthounds and modern wolves. (*c*) *D*-statistics comparing African dogs to Eurasia ancient wolves.

Each ancient wolf genome was included in TreeMix analysis (supplementary fig. S7, Supplementary Material online). The results identified two distinct patterns: 1) The phylogenetic tree reflected the patterns observed in our previous findings, indicating gene flow from ancient wolves to African native sighthounds and Chinese village dogs (fig. 2a); 2) Middle Eastern village dogs were located at the root of the African dog lineage, with gene flow detected from ancient wolves to the ancestors of the Middle Eastern village dogs, African dogs, and Chinese village dogs (fig. 2b and supplementary fig. S8, Supplementary Material online). We further examined gene flow between all sighthounds and ancient wolves (supplementary fig. S9, Supplementary Material online) by using *D*-statistics. The results supported the occurrence of gene flow between African native sighthounds and ancient wolves ($|Z| > 3.05$; fig. 2c and supplementary fig. S10, Supplementary Material online). Furthermore, analysis based on *D* (ancient wolves, modern wolves, African native sighthounds, and foxes) revealed gene flow was detected between ancient wolves and African native sighthounds,

rather than modern wolves ($|Z| > 3.19$; fig. 2c and supplementary fig. S11, Supplementary Material online).

We also performed Patterson's *f3*-test and *D*-statistics to examine admixture and gene flow among sighthound populations (Reich et al. 2009). The *f3*-test results revealed that African native sighthounds formed from the admixture of African village dogs and the other four sighthound populations ($Z \leq -7.41$; supplementary table S3, Supplementary Material online). This hybridization likely contributed to the closer genetic proximity of African native sighthounds and other dogs being compared with African village dogs, as observed in the PCA results, and this is also a possible reason why African village dogs did not be the background branch of African native sighthounds in phylogenetic tree. *D*-statistics revealed gene flow between African native sighthounds and other sighthounds ($Z \leq -23.30$; supplementary table S4, Supplementary Material online). Also, European sighthounds were detected to have gene flows with other sighthound populations ($Z \leq -4.72$; supplementary table S4, Supplementary Material online). Moreover, we evaluated the genetic components of the three sighthounds by using

RFMix (Maples et al. 2013) (fig. 1c). We found that African native sighthounds contained 16.93% bloodline from Middle Eastern sighthounds and 10.46% from European sighthounds (supplementary table S5, Supplementary Material online). There was 11.01% introgression into European sighthounds from Borzoi (supplementary table S6, Supplementary Material online). Additionally, Middle Eastern sighthounds contained 14.29% bloodline from European sighthounds, 8.08% bloodline from African native sighthounds, and 6.35% bloodline from Borzoi (supplementary table S7, Supplementary Material online).

To identify the ancestral sources of sighthounds, we used the qpWave test in ADMIXTOOLS (Patterson et al. 2012). Results indicated the presence of at least five genetic streams contributing to the sighthounds (rank = 4, P = 1). (supplementary table S8, Supplementary Material online). To further validate these findings, we used fastsimcoal2 (Excoffier et al. 2013) to infer the demographic history of canine lineages based on two-dimensional site frequency spectra. We simulated four single sighthound origination models, including Africa-origination, Europe-origination, Middle-East-origination, and Russia-origination, as well as a multiple origination model incorporating gene flow based on RFMix measurements. The highest median likelihood occurred in the multiple origination models, supporting the topological structure of the neighbor-joining tree and suggesting unique origins in different sighthound groups (supplementary fig. S12, Supplementary Material online).

We also investigated identical by descent (IBD) sharing among the different populations (supplementary fig. S13, Supplementary Material online). In the 1,453 IBD segments detected using Refined IBD (Browning and Browning 2013), the highest level of IBD sharing was observed between the Borzoi and Chortai breeds, accounting for 3.37% of the total IBD segments, with an average IBD segments length of 524,975 bp. Interestingly, no IBD segments shared by all sighthound breeds were found.

Artificial Selection in Sighthounds

It is interesting to observe that sighthounds from diverse origins share similar phenotypes, behaviors, and physiological traits, implying the selection of different genes from the same pathway. To unravel the genomic basis underlying these shared complex traits of sighthounds, we employed three approaches, that is, F-statistic (Fst), cross-population extended haplotype homozygosity (XP-EHH), and cross-population number of segregating sites by length (XP-nSL), to identify genomic regions displaying high population differentiation between sighthounds and their sympatric village dogs. Genomic regions exhibiting the top 1% of Fst values and empirical P < 0.01 values in both XP-EHH and XP-nSL analyses were selected for gene annotation. Genes that passed all three thresholds were selected as candidate genes. In total, we identified 17 positively selected genes (PSGs) in African sighthounds, 27 PSGs in European sighthounds, and 54 PSGs in Middle Eastern sighthounds. To differentiate

between signals of credible positive selection and those influenced by other factors that can cause false positive, we conducted sequence simulation based on the best model generated using fastsimcoal2. Comparing the candidate PSGs with the simulated sequence, we observed an obvious difference (supplementary fig. S14, Supplementary Material online). Given the absence of common PSGs across the three sighthound populations, we attempted to identify shared biological pathways and functions within the sighthound populations. This approach was utilized to overcome the heterogeneity among the populations and identify common biological processes from different PSGs (fig. 3 and supplementary tables S9, and S10, Supplementary Material online). After excluding three novel genes, a total of 95 genes were pooled, demonstrating significant enrichment in the top 16 gene ontology (GO) summary terms (−log P > 2.01; supplementary table S10, Supplementary Material online), with contributions from different populations. Among the top 16 terms, ten contained PSGs from African, European, and Middle Eastern populations. To visualize the relationships among these terms, a network was constructed based on their category clustering (supplementary fig. S15a, Supplementary Material online) and the contribution of genes from each population (supplementary fig. S15b, Supplementary Material online).

The pooled PSGs were enriched in various categories associated with the hematological and nervous systems, including positive regulation of blood pressure (GO: 0045777) and axon development (GO: 0061564). Notably, the heart-related summary term "Regulation of release of sequestered calcium ion into cytosol" (GO: 0051279) has member terms "regulation of heart rate" (GO: 0002027), "regulation of heart contraction" (GO: 0008016), and "heart process" (GO: 0003015), included PSGs from three population. Within this summary term, two notable PSGs from the Middle Eastern were identified, that is, estrogen receptor 1 (ESR1) and Janus kinase 2 (JAK2). ESR1 is a pleiotropic gene associated with bone mineral density and osteoporosis (Becherini et al. 2000; Ongphiphadhanakul et al. 2000; Albagha et al. 2001; Weise et al. 2001; Kemp et al. 2017; Montazeri-Najafabady et al. 2019), body fat distribution (Tchernof et al. 2000; Gu et al. 2009), and long legs in dogs (Plassais et al. 2019). JAK2 is involved in hematopoiesis (Perner et al. 2019) and enhances muscle repair and regeneration when inhibited (Price et al. 2014). In addition to ESR1 and JAK2, another PSG enriched in GO: 0051279 from the Middle Eastern population was β1-adrenergic receptor (ADRB1), which constitutes the majority of cardiac β-adrenergic receptors (Caro and Schnös 1966) and controls catecholamine-dependent changes in heart rate, force, and contracted speed of the heart by the second messenger cyclic adenosine monophosphate (cAMP) (Engelhardt et al. 1999; Nikolaev et al. 2006; Gorelik et al. 2013).

PSGs identified in European sighthounds and enriched in GO: 0051279 included Parkin RBR E3 Ubiquitin Protein Ligase (PRKN) and protein kinase C-epsilon

Fig. 3. Positive selection in sighthounds from Africa, Europe, and Middle East. (*a*–*c*) Genome-wide original Fst and empirical *P* values of XP-EHH and XP-nSL for African native sighthound. We highlighted candidate genes that above the cutoff in all three methods, and genes mentioned in the main text are labeled. (*d*–*f*) Genome-wide original Fst and empirical *P* values of XP-EHH and XP-nSL for European sighthound. (*g*–*i*) Genome-wide original Fst and empirical *P* values of XP-EHH and XP-nSL for Middle Eastern sighthounds.

(*PRKCE*). Notably, *PRKN* contains skeletal muscle/myoblast-specific enhancer chromatin, a myoblast-specific antisense RNA, and brain-specific enhancer chromatin (Ehrlich et al. 2022). In addition, *PRKCE* is an isoform of the large protein kinase C (*PKC*) family of enzymes that regulates cardiac muscle contraction, as well as cardiac cell energy production and metabolism (Scruggs et al. 2016).

For the same term, the African native sighthounds exhibited the presence of calcium/calmodulin-dependent protein kinase 2 delta (*CAMK2D*) enriched in "regulation of muscle cell apoptotic process" (GO: 0010660). *CAMK2D* is an isoform of calcium/calmodulin-dependent protein kinase 2 (*CAMK2*), which shows increased expression in skeletal muscle during exercise (Rose et al. 2006) and influences cardiac function (Zhang et al. 2003). The protein encoded by *CAMK2D* plays a functional role in regulating heart contractions (Kushnir et al. 2010).

T > C Mutation at chr1: g.42,177,149 Reduces *ESR1* Expression

Previous studies have indicated the core role of *ESR1* in the breeding process of sighthounds (Plassais et al. 2019;

Morrill et al. 2022). To identify significantly different sites between sighthound and nonsighthound dogs, we compared the allele frequency of *ESR1* SNPs using the chi-square test. Based on this analysis, we identified a SNP (chr1: g.42,177,149 T > C of CanFam3.1) in *ESR1* with significantly higher allele frequency ($-\log P > 15.65$) in sighthounds (allele frequency = 51.18%) than in other dogs (allele frequency = 7.28%). We predicted its possible transcription factor (TF) binding sites using the open-access JASPAR database (Portales-Casamar et al. 2010) and identified that signal transducer and activator of transcription 5 (*STAT5A*) binds to a specific site in *ESR1* (fig. 4*a*).

To test whether the T > C mutation at chr1: g.42,177,149 would regulate *ESR1* gene expression by affecting Stat5a binding, we generated plasmids containing the Stat5a binding region with wild type and mutation type and predicted *ESR1* promoter, and transient transfection was performed in H9C2 and A673 cell lines. After transfection of the H9C2 cell line (fig. 4*b*), the cloned region containing the predicted *ESR1* promoter (PGL3-*ESR1* promoter) showed 49.92% higher luciferase expression than the pGL3-basic plasmid, demonstrating the activity of the predicted *ESR1* promoter. Moreover,
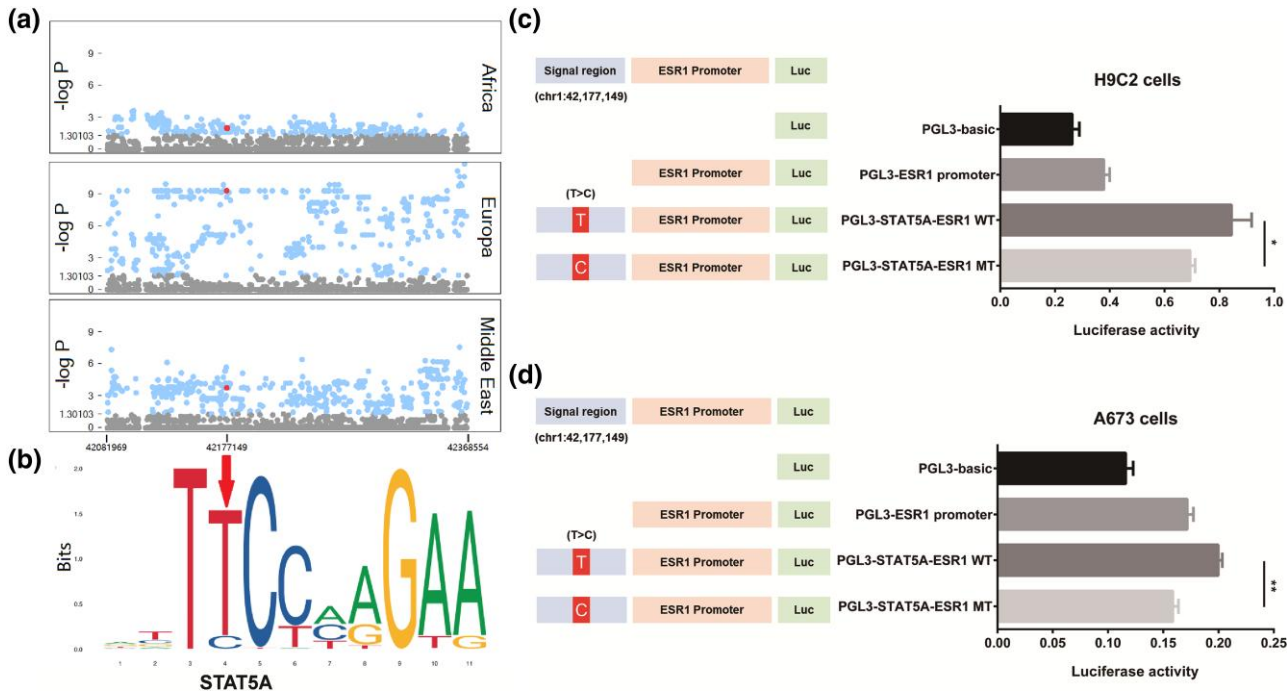
FIG. 4. Luciferase reporter on chr1: g.42,177,149 T > C of *ESR1*. (*a*) Fisher's exact test of site allele frequency in *ESR1* region of each comparison, with chr1: g.42,177,149 T > C (red dot) is beyond the significance level of 0.01 (−log P > 1.97) in all comparisons. (*b*) Sequence logo of the Stat5a-binding site on *ESR1* provided by JASPAR (https://jaspar.genereg.net/matrix/MA0519.1/); arrowhead points to chr1: g.42,177,149 T > C mutation position. (*c*) Luciferase reporter was applied to H9C2 cells, and *ESR1* expression in wild type (T) was significantly higher (*t*-test $P = 2.56 \times 10^{-2}$) than that in mutation type (C). (*d*) Luciferase reporter was applied to A673 cells, and ESR1 expression in wild type (T) was significantly higher (*t*-test $P = 2.22 \times 10^{-6}$) than that in mutation type (C).
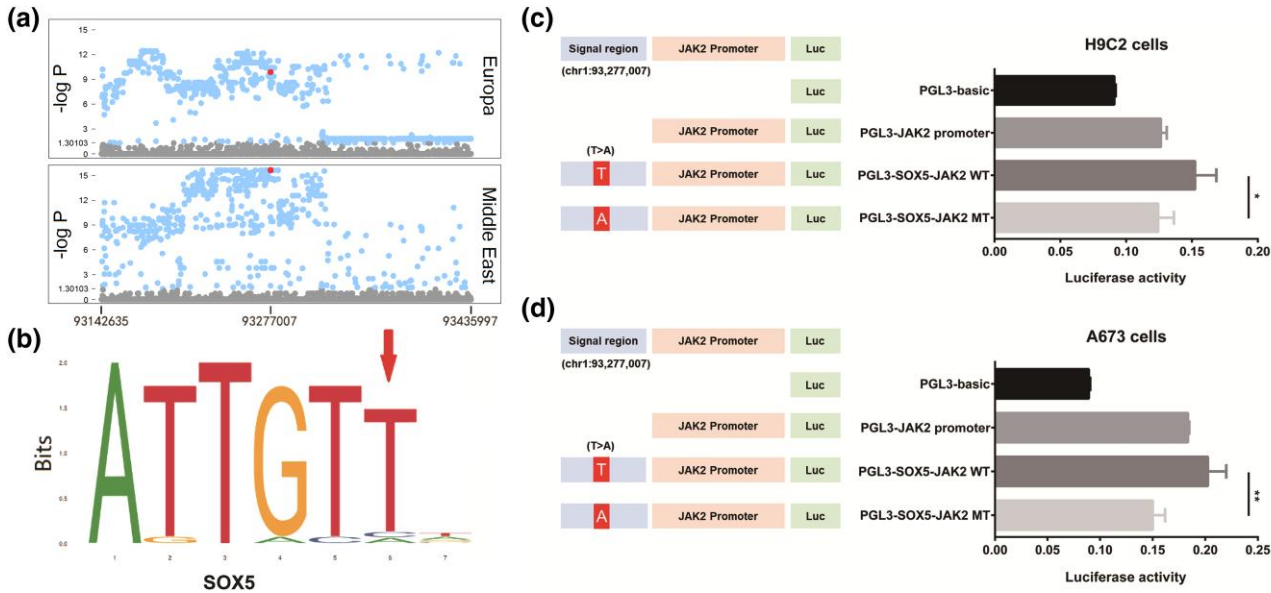

FIG. 5. Luciferase reporter on chr1 93,277,007 T > A of *JAK2*. (*a*) Fisher's exact test on-site allele frequency in the *JAK2* region of each comparison, with chr1 93,277,007 T > A (red dot) is beyond the significance level of 0.001 (−log P > 9.88) in all comparisons. (*b*) Sequence logo of the Sox5-binding site on *JAK2* provided by JASPAR (https://jaspar.genereg.net/matrix/MA0087.1/). (*c*) Luciferase reporter was applied to H9C2 cells, and *JAK2* expression in wild type (T) was significantly higher (*t*-test $P = 2.94 \times 10^{-2}$) than that in mutation type (A). (*d*) Luciferase reporter was applied to A673 cells, and *JAK2* expression in wild type (T) was significantly higher (*t*-test $P = 4.86 \times 10^{-3}$) than that in mutation type (A).

PGL3-*STAT5A-ESR1* showed higher transcription activity than the PGL3-*ESR1* promoter when the 300-bp region near the signal site was inserted, and PGL3-*STAT5A-ESR1* MT (chr1: g.42,177,149, C) showed 9.83% lower luciferase activity than PGL3-*STAT5A-ESR1* WT (chr1: g.42,177,149, T) ($P = 2.56 \times 10^{-2}$; fig. 4c). Similar results were found after transfection of the A673 cells (fig. 4d), further confirming the promoter activity of the predicted *ESR1* promoter. PGL3-*STAT5A-ESR1* MT (chr1: g.42,177,149, C) showed 20.51% lower promoter activity than PGL3-*STAT5A-ESR1* WT (chr1: g.42,177,149, T) ($P = 2.22 \times 10^{-6}$, fig. 4d). These results indicate that the T > C mutation at chr1: g.42,177,149 reduced *ESR1* expression by affecting its binding with *STAT5A*.

T > A Mutation at chr1: g.93,277,007 Reduces *JAK2* Expression

Distinct haplotype patterns were observed between sighthounds and nonsighthounds were found (supplementary fig. S16, Supplementary Material online) on *JAK2*. We identified a significant SNP (chr1: g.93,277,007 T > A of CanFam3.1) with a markedly higher allele frequency ($-\log P > 15.65$) in sighthounds (allele frequency = 60.61%) than in other dogs (allele frequency = 3.23%). This significance was maintained in both European and Middle Eastern sighthounds (fig. 5a). According to the predictions from JASPAR (Portales-Casamar et al. 2010) SRY-box transcription factor 5 (*SOX5*) was predicted to bind the site on *JAK2* (fig. 5b).

Transient transfection was also performed in the H9C2 and A673 cell lines (fig. 5b). The cloned region containing the predicted *JAK2* promoter (PGL3-JAK2 promoter) showed higher luciferase expression than the pGL3-basic plasmid, demonstrating the activity of the predicted *JAK2* promoter. Moreover, PGL3-*SOX5-JAK2* MT (chr1: g.93,277,007, A) showed lower promoter activity than PGL3-*SOX5-JAK2* WT (chr1: g.93,277,007, T) in the H9C2 ($P = 2.94 \times 10^{-2}$; fig. 5c) and A673 ($P = 4.86 \times 10^{-3}$; fig. 5d). These results indicate that the T > A mutation at chr1: g.93,277,007 reduced the expression of *JAK2* by affecting its binding with *SOX5*.

Discussion

Based on genomic analysis, we investigated the origin and artificial selection of sighthounds. Through techniques such as PCA, phylogenetic tree analysis, and population structure analysis, we determined that sighthounds were independently bred in Africa, Europe, and the Middle East, with admixture events. Furthermore, we explored positive selection signals in the three populations. Although the specific PSGs varied among the three groups, GO analysis of pooled PSGs revealed significant enrichment in pathways related to estrogen signaling, calcium transport, melanocortin receptor activity, and other biological processes primarily involved in bone mineral density, muscle repair and regeneration, and heart function. These findings shed light on the physiological mechanisms

contributing to the swiftness, strength, and unique appearance of sighthounds.

Multiple Origins of Sighthound Breeds

Genomic evidence suggests that the switch from hunting to agricultural pursuits may have initiated early breed formation; this could occur in multiple regions (Parker et al. 2017). Ancient dog breeds, such as Greyhounds and mastiffs, may have emerged during periods when human migration was challenging (Wayne and Ostrander 1999). Despite their ancient divergence, sighthounds share not only physical characteristics but also specific internal traits, such as high blood pressure (Bodey and Michell 1996) and cardiac properties (Locatelli et al. 2016). Based on these observations, three hypotheses can be proposed regarding the origin of sighthounds: 1) Sighthounds from different regions have no ancestral relationship but exhibit convergent selection, resulting in a similar phenotype; 2) sighthounds have a single common origin with shared ancestry, with their distinct genetic histories resulting in differentiated populations; and 3) sighthounds derived independently, with shared gene flow, rather than convergent selection, resulting in a similar phenotype. Our results showed that 128 sighthounds were geographically clustered together with African, European, and Middle Eastern village dogs based on the neighbor-joining phylogenic tree, PCA, and population structure analyses (fig. 1). The *QpWave* test and the different model tests support the multiple origin hypotheses. Phylogenic tree with gene flows by TreeMix, which included 31 modern and ancient wolves spanning from 5.2 to 93.6 kilo years ago (kya), corroborated the findings of the neighbor-joining tree (fig. 2a). Notably, no gene flow was detected among sighthound breeds in the TreeMix analysis, and there were no shared IBD segments observed across all sighthounds based on Refined IBD analysis. These findings provide additional support for the independent breeding of sighthounds in Africa, Europe, and the Middle East. While not all sighthound breeds are extremely ancient, it is possible that sighthounds, which originated before ancient human trade networks, had multiple origins due to extensive global interactions. Consequently, there may be no overlap in PSGs among the scattered sighthound populations across the three continents. However, the RFMix analysis results detected noticeable gene flow among sighthounds, indicating that the single origin hypothesis cannot be entirely ruled out. Repeated ancient backcrossing between foreign sighthounds and indigenous dogs can yield similar results to the close genetic relationships observed in the RFMix and phylogenetic trees.

Analyses using TreeMix and *D*-statistics revealed gene flow between African native sighthounds and ancient Eurasian wolves (fig. 2c and supplementary fig. S11, Supplementary Material online), it suggests a potential interaction between gray wolf outside of Africa and African native sighthound populations during sighthound's breeding process. This gene flow may explain

the abnormal position of African native sighthounds in both the PCA and phylogenetic tree. Interestingly, the characteristics of African native sighthounds, such as medium size, well-muscled physique, and exceptional running abilities, align with descriptions of "Africanis," an original African dog lineage believed to have ancient origins dating back at least 7 000 years, with an ancestry traced to prehistoric wolf packs in Arabia and India (Gallant 2002).

Genes under Positive Selection Contribute to Sighthound Phenotype

The GO terms enriched in the current study are consistent with the specific traits and abilities observed in sighthounds, such as their focusing ability, specialized cardiovascular fitness, and sport performance. In total, 64 distinct GO terms were enriched in the PSGs identified from the African, European, and Middle Eastern populations. These enriched categories, such as "axon development" (GO: 0061564) and "regulation of heart rate" (GO: 0002027), shed light on the fundamental biological processes that have contributed to the convergent evolution of functional syndromes in sighthounds. The enriched terms "heart development" (GO: 0007507) and "cell–cell adhesion" (GO: 0098609) have been reported in Saluki, a sighthound breed from the Middle East, using indels, copy number variation (CNV), and other structural variant regions (Amiri Ghanatsaman et al. 2020). Furthermore, our analysis revealed the selection of 13 members of the keratin family in Middle Eastern sighthounds, while other keratin family members were reported to be selected in Shaanxi sighthounds (Yang et al. 2019), which were grouped with European sighthound in our study. These findings suggest that phenotypes observed in sighthounds are linked to the complex GO network involving 64 pathways enriched in PSGs from different populations. Mutations in different genes involved in the same biology function categories may result in similar effects at the molecular level (Arendt and Reznick 2008; Wang et al. 2010; Losos 2011), indicating that breed development driven by artificial selection can affect the function of the same pathways and give rise to similar phenotypes, despite their independent breed histories.

ESR1 is a multifunctional gene (Cooke et al. 2017) that affects reproductive capacity (Muñoz et al. 2007), morphogenesis (Prins et al. 2006), breast cancer (Robinson et al. 2013), brain function (Rettberg et al. 2014), and behavior (Lee , Kim, et al. 2014; Pinsonneault et al. 2017), bone development (Weise et al. 2001; Khalid and Krum 2016), cardiovascular health (Zeng et al. 2016), and fat metabolism (Heine et al. 2000). Here, ESR1 was downregulated with a SNP (chr1: g.42,177,149 T > C), which may impact elongation of limb bones (Plassais et al. 2019) and contribute to the slender body observed in sighthounds. In addition, full deletion of ESR1 has been shown to increase bone mineral density in mice (Sims et al. 2003), with lower expression in skeletal muscle related to lean tissue and rapid growth (Voillet et al. 2018).

In our study, we observed a shared JAK2 haplotype among all sighthounds (supplementary fig. S12, Supplementary Material online). However, similar to ESR1, the effects of JAK2 can vary widely. Previous GWAS has linked JAK2 to herding behavior, which may play a role in suppressing aggressive behavior toward livestock (Shan et al. 2021), suggesting that JAK2 may affect the hunting behavior of sighthounds. Moreover, another GO term including JAK2 was enriched by PSGs from different populations and related to exercise: regulation of heart contraction (GO: 0008016). Special cardiovascular characteristic of sighthounds has been reported to be built by artificial selection (Cox et al. 1976a, 1976b). Also, STAT5B is under positive selection in Middle Eastern sighthounds. The JAK/STAT pathway regulates myogenic differentiation (Jang and Baik 2013), while the JAK2/STAT5 signaling pathway is related to hematopoietic function (Lim et al. 2011). This may contribute to sighthounds having a higher red blood cells count, as found in Greyhounds (Zaldivar-Lopez et al. 2011), providing the necessary energy for sprinting (Ilkiw et al. 1989; Rose and Bloomberg 1989). The changes of JAK2 observed in sighthounds likely have complex effects, but combined with the downregulation of JAK2, we inferred that this mutation protects blood vessels from cardiovascular damage (Kirabo et al. 2011; Zhang et al. 2020). Although experiments confirmed that the ESR1 and JAK2 mutations reduced their expression in vitro, their specific effects on phenotype remain unclear due to their pleiotropic nature and complex genome context in vivo.

Our study focused on sighthounds, an ancient group of dogs to investigate their origin and the genetic basis of their physiological characteristics. These traits, which were likely developed through early breeding efforts, would have facilitated hunting for primitive human populations and eased the transition from hunting-gathering to agriculture and animal husbandry. The widespread need for hunting in early human societies may explain the multiple origins of sighthounds, with similar selection pressure leading to convergent evolution. Our research revealed genes associated with the exceptional athletic performance and specialized phenotypes of sighthounds, shedding light on the genetic basis of their remarkable abilities.

Materials and Methods

Sample Collection

Samples from sighthounds were collected from 13 countries of potential sighthound origins (fig. 1a), with a focus on Asian regions as well as Europe and Africa. The samples included frozen blood or tissue stored in 95% alcohol. To understand the population history and identify PSGs, village dogs from Asia and Africa were also collected. Due to the scarcity of village dogs in Europe, other breeding dogs were selected as substitutes.

Whole-Genome Sequencing and SNP Calling

Samples were sequenced using the Illumina WGS workflow, and mapping was performed using the classical

BWA-MEM-Samtools-PicardTools (Li 2013) pipeline with the Canfam 3.1 reference. We used GATK gears to yield an analysis-ready SNP data set with the following filter parameters:

QD < 2.0 || FS > 60.0 || MQ < 40.0 || QUAL < 50.0 || MQRankSum < −12.5 || ReadPosRankSum < −8.0 || MQ0 ≥ 4 || ([MQ0/{1.0 * DP}] > 0.1) QD < 2.0 || FS > 200.0 || ReadPosRankSum < −20.0. SNPs on autosomes were used for subsequent workflow.

Population Structure and Phylogeny

We used Genome-wide Complex Trait Analysis (GCTA) (Yang et al. 2011) to perform PCA with whole-genome next-generation sequencing (NGS) data after filtration. A neighbor-joining tree was constructed using MEGA (Tamura et al. 2007). Structure analysis was conducted using ADMIXTURE (Alexander et al. 2009), with the same SNPs used for PCA.

For each population, θ_π was calculated using VCFtools (v0.1.13) with a 40-kb window (Danecek et al. 2011), and the Wilcoxon rank sum test was performed using the θ_π values with the built-in function in R.

We utilized ADMIXTOOLS (Reich et al. 2009) to conduct D-statistics and $f3$-tests. In the D-statistics test, we included the red fox (*Vulpes vulpes*) (Auton et al. 2013) as an outgroup, following the format D (Outgroup [P1 {P2, P3}]).

Difference in Diversity, ROH, and Inbreeding Coefficients between Native Sighthounds and Sighthounds Recognized in FCI or AKC

We categorized the sighthounds into different breeds and retained ten breeds that with a minimum of three samples each. To eliminate possible bias from different sample size in each group, we randomly select three samples from each breed for analyses of diversity, ROH, and inbreeding coefficient. Diversity was analyzed using VCFtools with a 40-kb window.

The ROH of sighthounds was calculated using PLINK v1.9 with the following filter parameters: −homozyg − homozyg-density 50 −homozyg-gap 1000 −homozyg-kb 200 −homozyg-window-snp 100 −homozyg-window-het 5.

The inbreeding coefficient (F_{ROH}) was determined by calculating the proportion of the genome covered by ROH. This was achieved by dividing the total length of ROH by the total autosomal length of the genome (2,203,764,842 bp).

IBD Mapping

We use the PLINK v1.9 with option "−genome" to identify the paired combination of individuals that PI_HAT > 0.2 and Z1 > 0.9, individuals in these pairs are removed for high kinship correlation. To detect shared IBD segments between pairs of individuals, we employed the stand-alone program Refined IBD (refined-ibd.17Jan20.102.jar) (Browning and Browning 2013). Analysis was conducted using default parameters; the physical map used in the analysis was based on Canfam3.1.

TreeMix between Sighthounds and Ancient Wolves

We downloaded a genomic data set comprised of 67 published ancient wolves and an additional genome sequence of a 70-ka dhole as the outgroup (Bergstrom et al. 2020). We then used snpAD to jointly estimate error rates and genotype frequency (Prüfer 2018). The ancient genome data set was combined with the sighthound data set using BCFtools (v1.8) (Danecek et al. 2021), with only shared genomic sites retained. To avoid the effects of ancient DNA damage, we restricted the D-statistics and TreeMix analyses into 7,075,777 transversion sites.

The sighthounds were divided into 14 groups based on breed information. Each ancient wolf was then separately added to the data set for TreeMix analysis, with SNPs detected in both sighthounds and ancient wolves used.

Gene Flow between Sighthounds and Modern Wolves

D-statistics was carried out based on breed to determine potential gene flow between sighthounds and modern wolf populations. Sighthounds and nonsighthounds from the same geographical location were pairwise analyzed to calculation D ([{sighthounds, village dog}, modern wolf], Fox) using the R package admixr.

Gene Flow between Sighthounds and Ancient Wolves

Based on the above data set, we calculated D ([{sighthound, village dog}, ancient wolf], Fox) for each ancient wolf and each sighthound breed using the R package admixr. With the same method, we calculated D ([{ancient wolf, modern wolf}, sighthound], Fox) to determine potential gene flow between sighthounds and ancient wolves against the background of modern wolves. To minimize false positives affected by ancient DNA damage, only transversion sites were input to test gene flow.

Demographic Model Testing

Based on population structure analysis, we grouped the samples into ten populations (wolf, Southeast Asian village dog, African village dog, African sighthound, Middle Eastern sighthound, Middle Eastern village dog, European breed dog, European sighthound, and Russian sighthound including Borzoi and Chortai) to generate a site frequency spectrum. After removing the sites with a high missing ratio (>80%), we thinned the data by retaining one SNP within 10 kb to reduce the effect of LD. Based on the fox genome (Auton et al. 2013), SNPs were unfolded as ancestral or derived. The site frequency spectrum was then calculated using easySFS (https://github.com/isaacovercast/easySFS). Subsequently, we determined the demographic history of dogs and wolves using fastsimcoal2 (v 3.7.9) (Excoffier et al. 2013). We set the nuclear mutation rate to 4×10^{-9} per site per generation (Raghavan et al. 2014; Pendleton et al. 2018) and assumed a generation time of 3 years. We then performed 50 replicate runs for each model and each replicate using 100,000 coalescent

simulations and ran 40 optimization cycles. The best-fit model was selected based on the highest mean MaxEstLhood.

Coalescent Simulation

Parameters outputted by the best run of fastsimcoal2 (v 3.7.9), which has the highest MaxObsLhood, were adjusted to adjust *ms* program (Hudson 2002). We then use *ms* to simulate 200-kb sequence 20,000 times. The average number of SNPs on a 200-kb sequence was calculated as the product of SNP density and sequence length, that is, 26,547,340 SNPs/2,410,976,875 bp $\times$ 200,000 bp $\approx$ 2,202 SNPs. Therefore, a 200-kb sequence for every haplotypes involved in the selection analysis was simulated 20,000 times using the following script:

ms 522 1 -t 64 -s 2202 -I 10 62 66 24 102 30 30 50 86 26 46 -n 1 19.9724 -n 2 5.37545 -n 3 2.5428 -n 4 1.2108 -n 5 3.9399 -n 6 1.65705 -n 7 0.07 -n 8 4.90885 -n 9 1.42355 -n 10 2.109 -m 4 3 6078.1274 -m 6 4 3533.1232 -m 7 4 2603.9501 -m 6 5 4726.7923 -m 4 6 2459.0507 -m 4 7 9609.5474 -m 6 7 5839.3261 -m 4 9 1094.5907 -m 7 9 1369.8888 -m 4 10 2487.3236 -m 7 10 491.7643 -en 0.068687 10 0.249762 -en 0.068687 9 0.282875 -en 0.22578 8 0.765 -en 0.112096 7 0.0140375 -en 0.0129698 6 0.224675 -en 0.45937 5 0.399487 -en 0.001852832 4 0.191812 -en 0.45937 3 0.955812 -en 0.91053 2 0.085475 -eg 0.0440709 10 0.00134835 -eg 0.0026997 9 0.00406776 -eg 0.178666 8 -0.000080321 -eg 0.0075436 7 0.0651426 -eg 0.012969 6 0.00236844 -eg 0.012969 5 0.00229158 -eg 0.00185283 4 -0.00593132 -eg 0.00185283 3 -0.0374482 -eg 0.8867125 2 -0.000022149 -eg 0.99999 1 -0.000012412 -ej 0.001853 3 4 -ej 0.01297 5 6 -ej 0.068687 10 9 -ej 0.112096 7 9 -ej 0.225781 8 9 -ej 0.45937 4 6 -ej 0.478692 6 9 -ej 0.910535 2 9 -ej 0.99999 9 1 -p 6.

Population Differentiation

Fst analysis was performed using VCFtools (v0.1.13) with a 40-kb window and 20-kb step (Danecek et al. 2011). We selected the top 1% of regions for gene annotation. We calculated XP-EHH and XP-nSL between sighthounds and their sympatric indigenous dogs using selscan (v1.3.0) (Sabeti et al. 2007; Szpiech and Hernandez 2014). The empirical *P* values of XP-EHH and XP-nSL were calculated following the method as previously studied (Lee, Abecasis, et al. 2014): 1) The genome was divided into nonoverlapping 50-kb windows, and the maximum XP-EHH or XP-nSL score of all SNVs within each window was used as a summary statistic. 2) Genomic windows were binned based on the number of SNVs they contained (in increments of 200 SNVs), with all windows containing 800 or more SNVs combined into a single bin. 3) Within each bin, the empirical *P* value was calculated for each window (i), representing the fraction of windows within the bin that have a statistic greater than that of window (i), providing a measure of statistical significance. Genomic regions with $P < 0.01$ were considered for gene annotation. Gene sets were downloaded from Ensembl (version

CanFam3.1.104). Allele frequency differences were tested using Fisher's exact test.

Go Enrichment Analysis

After obtaining overlapping PSGs from the three selection signal tests (Fst, XPEHH, and XP-nSL) in each population, we performed GO enrichment at Metascape (Zhou et al. 2019) (http://metascape.org/gp/index.html) with a pooled gene set combining all PSGs from the three comparisons. Using default pathway and process enrichment settings (Min Overlap = 3, P Value Cutoff = 0.01, Min Enrichment = 1.5), four items were calculated (GO molecular functions, GO biological processes, KEGG pathway, and GO cellular components).

Experiment
Cell Culture

H9c2 rat heart myocytes and A673 human muscle Ewing's sarcoma cell lines were obtained from the Chinese Academy of Sciences, Typical Culture Preservation Committee Cell Bank (Shanghai, China). The cells were routinely grown in Dulbecco's Modified Eagle's Medium (DMEM) (Thermo Fisher Scientific, Waltham, MA, USA) with 10% fetal bovine serum (FBS) (Thermo Fisher Scientific). Cells were cultured at 37 °C in 5% CO_2 in a humidified incubator (Thermo Fisher Scientific).

Luciferase Reporter Assay

To determine the biological function of the selected signal site in the *ESR1* gene, which binds to *STAT5A* TF, the 300-bp region near the signal site and predicted *ESR1* promoter were selected to insert PGL3-basic and construct an expression vector (Tsingke Biological Technology, Beijing, China). An expression vector of the *JAK2* promoter and TF SOX5-binding region was also constructed. All plasmids used for reporter assays were confirmed by sequencing. Primer sequences are available in supplementary table S11, Supplementary Material online.

For reporter assays, constructs were transfected into H9c2 and A673 cells using ViaFect transfection reagent (Promega, Madison, WI, USA), and luciferase expression was normalized to *Renilla* luciferase expression. After 24 h of transfection, cells were harvested, and luciferase activity was measured using the Dual-Luciferase Reporter Assay System (Promega) according to the manufacturer's protocol. Luminescence signals were captured in a Glomax 96 Microplate Luminometer (Promega). Data represent at least six independent experiments. Student's two-tailed *t*-test was used to determine statistical significance, and the null hypothesis was rejected at $P > 0.05$.

Supplementary Material

Supplementary data are available at *Molecular Biology and Evolution* online.

Acknowledgments

Author Contributions

Y.-P.Z., G.-D.W., and P.S. supervised and designed the research. Y.-H.L., M.-T.D., and W.-L.L. analyzed the data. J.-X.L., X.Z.H., and G.L.X. performed functional assay. A.C.A., M.-S.P., A.E., Z.A.G., S.C.O., O.J.S., W.-W.Z., C.S., W.-K.Y., M.J.K., H.L., and A.D.P. provided the blood samples of canines. W.-L.L. carried out data submission. A.C.A., M.-S.P., X.Z.H., Z.A.G., A.E., A.D.P., P.S., G.-D.W., Y.-P.Z., and P.M.D. helped perform analysis with constructive discussions. Y.H.L., M.T.D., W.-L.L., and J.-X.L. wrote the manuscript. A.-E., A.D.P, Y.-P.Z., G.-D.W., and P.S. revised the manuscript.

Ethics Approval

This work was approved by the Institutional Animal Care and Use Committee (Kunming Institute of Zoology, approval ID: SMKX-20160805-118), and blood samples were collected under the permission of the County Administrative Board of Southern Finland (ESAVI/7482/04.10.07/2015).

Data Availability

The raw sequence data from this study have been submitted to the GSA (http://gsa.big.ac.cn/) under accession PRJCA001011.

References

Adeola AC, Ommeh SC, Song JJ, Olaogun SC, Sanke OJ, Yin TT, Wang GD, Wu SF, Zhou ZY, Lichoti JK, et al. 2017. A cryptic mitochondrial DNA link between North European and West African dogs. *J Genet Genomics.* **44**:163–170.

Albagha OM, McGuigan FE, Reid DM, Ralston SH. 2001. Estrogen receptor alpha gene polymorphisms and bone mineral density: haplotype analysis in women from the United Kingdom. *J Bone Miner Res.* **16**:128–134.

Alexander DH, Novembre J, Lange K. 2009. Fast model-based estimation of ancestry in unrelated individuals. *Genome Res.* **19**:1655–1664.

Amiri Ghanatsaman Z, Wang G-D, Asadollahpour Nanaei H, Asadi Fozi M, Peng M-S, Esmailizadeh A, Zhang Y-P. 2020. Whole genome resequencing of the Iranian native dogs and wolves to unravel variome during dog domestication. *BMC Genomics* **21**:207.

Arendt J, Reznick D. 2008. Convergence and parallelism reconsidered: what have we learned about the genetics of adaptation? *Trends Ecol Evol.* **23**:26–32.

Auton A, Rui Li Y, Kidd J, Oliveira K, Nadel J, Holloway JK, Hayward JJ, Cohen PE, Greally JM, Wang J, et al. 2013. Genetic recombination is targeted towards gene promoter regions in dogs. *PLoS Genet.* **9**:e1003984.

Becherini L, Gennari L, Masi L, Mansani R, Massart F, Morelli A, Falchetti A, Gonnelli S, Fiorelli G, Tanini A, et al. 2000. Evidence of a linkage disequilibrium between polymorphisms in the human estrogen receptor alpha gene and their relationship to bone mass variation in postmenopausal Italian women. *Hum Mol Genet.* **9**:2043–2050.

Bergstrom A, Frantz L, Schmidt R, Ersmark E, Lebrasseur O, Girdland-Flink L, Lin AT, Stora J, Sjogren KG, Anthony D, et al. 2020. Origins and genetic legacy of prehistoric dogs. *Science* **370**:557–564.

Bergstrom A, Stanton DWG, Taron UH, Frantz L, Sinding MS, Ersmark E, Pfrengle S, Cassatt-Johnstone M, Lebrasseur O, Girdland-Flink L, et al. 2022. Grey wolf genomic history reveals a dual ancestry of dogs. *Nature* **607**:313–320.

Bodey AR, Michell AR. 1996. Epidemiological study of blood pressure in domestic dogs. *J Small Anim Pract.* **37**:116–125.

Boyko AR, Boyko RH, Boyko CM, Parker HG, Castelhano M, Corey L, Degenhardt JD, Auton A, Hedimbi M, Kityo R, et al. 2009. Complex population structure in African village dogs and its implications for inferring dog domestication history. *Proc Natl Acad Sci U S A.* **106**:13903–13908.

Browning BL, Browning SR. 2013. Improving the accuracy and efficiency of identity-by-descent detection in population data. *Genetics* **194**:459–471.

Brunson DB, Hogan KJ. 2004. Malignant hyperthermia: a syndrome not a disease. *Vet Clin North Am Small Anim Pract.* **34**:1419–1433.

Caro LG, Schnös M. 1966. The attachment of the male-specific bacteriophage F1 to sensitive strains of Escherichia coli. *Proc Natl Acad Sci U S A.* **56**:126–132.

Como D. 2004. *Sighthounds afield—the complete guide to sighthounds & amateur performance events, with a comprehensive chapter on adopted ex-racing greyhounds.* Bloomington (IN): AuthorHouse.

Cooke PS, Nanjappa MK, Ko C, Prins GS, Hess RA. 2017. Estrogens in male physiology. *Physiol Rev.* **97**:995–1043.

Court MH. 1999. Anesthesia of the sighthound. *Clin Tech Small Anim Pract.* **14**:38–43.

Cox RH, Peterson LH, Detweiler DK. 1976a. Comparison of arterial hemodynamics in the mongrel dog and the racing greyhound. *Am J Physiol.* **230**:211–218.

Cox RH, Peterson LH, Detweiler DK. 1976b. Hemodynamic responses to stellate ganglion stimulation in mongrels and greyhounds. *Am J Physiol.* **231**:1062–1067.

Danecek P, Auton A, Abecasis G, Albers CA, Banks E, DePristo MA, Handsaker RE, Lunter G, Marth GT, Sherry ST, et al. 2011. The variant call format and VCFtools. *Bioinformatics* **27**:2156–2158.

Danecek P, Bonfield JK, Liddle J, Marshall J, Ohan V, Pollard MO, Whitwham A, Keane T, McCarthy SA, Davies RM, et al. 2021. Twelve years of SAMtools and BCFtools. *Gigascience* **10**:1–4.

Ding ZL, Oskarsson M, Ardalan A, Angleby H, Dahlgren LG, Tepeli C, Kirkness E, Savolainen P, Zhang YP. 2012. Origins of domestic dog in southern East Asia is supported by analysis of Y-chromosome DNA. *Heredity (Edinb).* **108**:507–514.

Dutrow EV, Serpell JA, Ostrander EA. 2022. Domestic dog lineages reveal genetic drivers of behavioral diversification. *Cell* **185**: 4737–4755.e18.

Ehrlich KC, Deng HW, Ehrlich M. 2022. Epigenetics of mitochondria-associated genes in striated muscle. *Epigenomes.* **6**:1–1.

Engelhardt S, Hein L, Wiesmann F, Lohse MJ. 1999. Progressive hypertrophy and heart failure in β₁-adrenergic receptor transgenic mice. *Proc Natl Acad Sci U S A.* **96**:7059–7064.

Excoffier L, Dupanloup I, Huerta-Sanchez E, Sousa VC, Foll M. 2013. Robust demographic inference from genomic and SNP data. *PLoS Genet.* **9**:e1003905.

Fan Z, Silva P, Gronau I, Wang S, Armero AS, Schweizer RM, Ramirez O, Pollinger J, Galaverni M, Ortega Del-Vecchyo D, et al. 2016. Worldwide patterns of genomic variation and admixture in gray wolves. *Genome Res.* **26**:163–173.

Frantz LA, Mullin VE, Pionnier-Capitan M, Lebrasseur O, Ollivier M, Perri A, Linderholm A, Mattiangeli V, Teasdale MD, Dimopoulos EA, et al. 2016. Genomic and archaeological evidence suggest a dual origin of domestic dogs. *Science* **352**:1228–1231.

Freedman AH, Gronau I, Schweizer RM, Ortega-Del Vecchyo D, Han E, Silva PM, Galaverni M, Fan Z, Marx P, Lorente-Galdos B, et al. 2014. Genome sequencing highlights the dynamic early history of dogs. *PLoS Genet.* **10**:e1004016.

Gallant J. 2002. *The story of the African dog.* Scottsville: University of Natal Press.

Gopalakrishnan S, Sinding MS, Ramos-Madrigal J, Niemann J, Samaniego Castruita JA, Vieira FG, Carøe C, Montero MM, Kuderna L, Serres A, et al. 2018. Interspecific gene flow shaped the evolution of the genus *Canis. Curr Biol.* **28**:3441–3449.e5.

Gorelik J, Wright PT, Lyon AR, Harding SE. 2013. Spatial control of the βAR system in heart failure: the transverse tubule and beyond. *Cardiovasc Res.* **98**:216–224.

Gottipati S, Arbiza L, Siepel A, Clark AG, Keinan A. 2011. Analyses of X-linked and autosomal genetic variation in population-scale whole genome sequencing. *Nat Genet.* **43**:741–743.

Gou X, Wang Z, Li N, Qiu F, Xu Z, Yan D, Yang S, Jia J, Kong X, Wei Z, et al. 2014. Whole-genome sequencing of six dog breeds from continuous altitudes reveals adaptation to high-altitude hypoxia. *Genome Res.* **24**:1308–1315.

Gu JM, Xiao WJ, He JW, Zhang H, Hu WW, Hu YQ, Li M, Liu YJ, Fu WZ, Yu JB, et al. 2009. Association between VDR and ESR1 gene polymorphisms with bone and obesity phenotypes in Chinese male nuclear families. *Acta Pharmacol Sin.* **30**: 1634–1642.

Hancock D. 2012. *Sighthounds: their form, their function and their future.* Ramsbury: Crowood Press.

Heilmann RM, Grutzner N, Iazbik MC, Lopes R, Bridges CS, Suchodolski JS, Couto CG, Steiner JM. 2017. Hyperhomocysteinemia in greyhounds and its association with hypofolatemia and other clinicopathologic variables. *J Vet Intern Med.* **31**:109–116.

Heine PA, Taylor JA, Iwamoto GA, Lubahn DB, Cooke PS. 2000. Increased adipose tissue in male and female estrogen receptor-alpha knockout mice. *Proc Natl Acad Sci U S A.* **97**: 12729–12734.

Hudson RR. 2002. Generating samples under a Wright–Fisher neutral model of genetic variation. *Bioinformatics.* **18**:337–338.

Ilkiw JE, Davis PE, Church DB. 1989. Hematologic, biochemical, blood-gas, and acid-base values in greyhounds before and after exercise. *Am J Vet Res.* **50**:583–586.

Jang YN, Baik EJ. 2013. JAK-STAT pathway and myogenic differentiation. *JAKSTAT.* **2**:e23282.

Kemp JP, Morris JA, Medina-Gomez C, Forgetta V, Warrington NM, Youlten SE, Zheng J, Gregson CL, Grundberg E, Trajanoska K, et al. 2017. Identification of 153 new loci associated with heel bone mineral density and functional involvement of GPC6 in osteoporosis. *Nat Genet.* **49**:1468–1475.

Kent M, Glass EN, Haley AC, March P, Rozanski EA, Galban EM, Bertalan A, Platt SR. 2014. Ischemic stroke in Greyhounds: 21 cases (2007-2013). *J Am Vet Med Assoc.* **245**:113–117.

Khalid AB, Krum SA. 2016. Estrogen receptors alpha and beta in bone. *Bone* **87**:130–135.

Kim J, Williams FJ, Dreger DL, Plassais J, Davis BW, Parker HG, Ostrander EA. 2018. Genetic selection of athletic success in sport-hunting dogs. *Proc Natl Acad Sci U S A.* **115**:E7212–E7221.

Kirabo A, Oh SP, Kasahara H, Wagner KU, Sayeski PP. 2011. Vascular smooth muscle Jak2 deletion prevents angiotensin II-mediated neointima formation following injury in mice. *J Mol Cell Cardiol.* **50**:1026–1034.

Koepfli KP, Pollinger J, Godinho R, Robinson J, Lea A, Hendricks S, Schweizer RM, Thalmann O, Silva P, Fan Z, et al. 2015. Genome-wide evidence reveals that African and eurasian golden jackals are distinct Species. *Curr Biol.* **25**:2158–2165.

Kushnir A, Shan J, Betzenhauser MJ, Reiken S, Marks AR. 2010. Role of CaMKIIdelta phosphorylation of the cardiac ryanodine receptor in the force frequency relationship and heart failure. *Proc Natl Acad Sci U S A.* **107**:10274–10279.

Lee S, Abecasis GR, Boehnke M, Lin X. 2014. Rare-variant association analysis: study designs and statistical tests. *Am J Hum Genet.* **95**: 5–23.

Lee H, Kim DW, Remedios R, Anthony TE, Chang A, Madisen L, Zeng H, Anderson DJ. 2014. Scalable control of mounting and attack by Esr1+ neurons in the ventromedial hypothalamus. *Nature* **509**:627–632.

Li H. 2013. Aligning sequence reads, clone sequences and assembly contigs with BWA-MEM. arXiv: 1303.3997. https://doi.org/10.48550/arXiv.1303.3997, 26 May 2013, preprint: not peer reviewed.

Lim J, Jeong SJ, Koh W, Han I, Lee HJ, Kwon TR, Jung JH, Kim JH, Lee HJ, Lee EO, et al. 2011. JAK2/STAT5 signaling pathway mediates Bojungbangdocktang enhanced hematopoiesis. *Phytother Res.* **25**:329–337.

Liu YH, Wang L, Xu T, Guo X, Li Y, Yin TT, Yang HC, Yang H, Adeola AC, Sanke OJ, et al. 2018. Whole-genome sequencing of African dogs provides insights into adaptations against tropical parasites. *Mol Biol Evol.* **35**:287–298.

Locatelli C, Spalla I, Zanaboni AM, Brambilla PG, Bussadori C. 2016. Assessment of right ventricular function by feature-tracking echocardiography in conscious healthy dogs. *Res Vet Sci.* **105**: 103–110.

Losos JB. 2011. Convergence, adaptation, and constraint. *Evolution.* **65**:1827–1840.

Maples BK, Gravel S, Kenny EE, Bustamante C. 2013. RFMix: a discriminative modeling approach for rapid and robust local-ancestry inference. *Am J Hum Genet.* **93**:278–288.

Marsden CD, Ortega-Del Vecchyo D, O'Brien DP, Taylor JF, Ramirez O, Vila C, Marques-Bonet T, Schnabel RD, Wayne RK, Lohmueller KE. 2016. Bottlenecks and selective sweeps during domestication have increased deleterious genetic variation in dogs. *Proc Natl Acad Sci U S A.* **113**:152–157.

McGreevy PD, Georgevsky D, Carrasco J, Valenzuela M, Duffy DL, Serpell JA. 2013. Dog behavior co-varies with height, bodyweight and skull shape. *PLoS One* **8**:e80529.

Meisel RP, Connallon T. 2013. The faster-X effect: integrating theory and data. *Trends Genet.* **29**:537–544.

Montazeri-Najafabady N, Dabbaghmanesh MH, Mohammadian Amiri R, Mirzai Z. 2019. Influence of estrogen receptor alpha polymorphism on bone mineral density in Iranian children. *Hum Hered.* **84**:82–89.

Morrill K, Hekman J, Li X, McClure J, Logan B, Goodman L, Gao M, Dong Y, Alonso M, Carmichael E, et al. 2022. Ancestry-inclusive dog genomics challenges popular breed stereotypes. *Science* **376**:eabk0639.

Muñoz G, Ovilo C, Estellé J, Silió L, Fernández A, Rodriguez C. 2007. Association with litter size of new polymorphisms on ESR1 and

ESR2 genes in a Chinese–European pig line. *Genet Sel Evol.* **39**: 195–206.

Nikolaev VO, Bünemann M, Schmitteckert E, Lohse MJ, Engelhardt S. 2006. Cyclic AMP imaging in adult cardiac myocytes reveals far-reaching β_1-adrenergic but locally confined β_2-adrenergic receptor-mediated signaling. *Circ Res.* **99**:1084–1091.

Ongphiphadhanakul B, Chanprasertyothin S, Payatikul P, Tung SS, Piaseu N, Chailurkit L, Chansirikarn S, Puavilai G, Rajatanavin R. 2000. Oestrogen-receptor-alpha gene polymorphism affects response in bone mineral density to oestrogen in post-menopausal women. *Clin Endocrinol (Oxf).* **52**:581–585.

Parker HG, Dreger DL, Rimbault M, Davis BW, Mullen AB, Carpintero-Ramirez G, Ostrander EA. 2017. Genomic analyses reveal the influence of geographic origin, migration, and hybridization on modern dog breed development. *Cell Rep.* **19**:697–708.

Parker HG, Kim LV, Sutter NB, Carlson S, Lorentzen TD, Malek TB, Johnson GS, DeFrance HB, Ostrander EA, Kruglyak L. 2004. Genetic structure of the purebred domestic dog. *Science* **304**: 1160–1164.

Patterson N, Moorjani P, Luo Y, Mallick S, Rohland N, Zhan Y, Genschoreck T, Webster T, Reich D. 2012. Ancient admixture in human history. *Genetics* **192**:1065–1093.

Pendleton AL, Shen F, Taravella AM, Emery S, Veeramah KR, Boyko AR, Kidd JM. 2018. Comparison of village dog and wolf genomes highlights the role of the neural crest in dog domestication. *BMC Biol.* **16**:64.

Perner F, Perner C, Ernst T, Heidel FH. 2019. Roles of JAK2 in aging, inflammation, hematopoiesis and malignant transformation. *Cells.* **8**:854–854.

Petr M, Vernot B, Kelso J. 2019. *Admixr*—R package for reproducible analyses using ADMIXTOOLS. *Bioinformatics* **35**:3194–3195.

Pinsonneault JK, Frater JT, Kompa B, Mascarenhas R, Wang D, Sadee W. 2017. Intronic SNP in ESR1 encoding human estrogen receptor alpha is associated with brain ESR1 mRNA isoform expression and behavioral traits. *PLoS One* **12**:e0179020.

Plassais J, Kim J, Davis BW, Karyadi DM, Hogan AN, Harris AC, Decker B, Parker HG, Ostrander EA. 2019. Whole genome sequencing of canids reveals genomic regions under selection and variants influencing morphology. *Nat Commun.* **10**:1489.

Pols S, Henneberg M, Norris R. 2016. Cranial arterial patterning in greyhounds: another case of internal intraspecific variation. *Anat Histol Embryol.* **45**:161–172.

Portales-Casamar E, Thongjuea S, Kwon AT, Arenillas D, Zhao X, Valen E, Yusuf D, Lenhard B, Wasserman WW, Sandelin A. 2010. JASPAR 2010: the greatly expanded open-access database of transcription factor binding profiles. *Nucleic Acids Res.* **38**: D105–D110.

Price FD, von Maltzahn J, Bentzinger CF, Dumont NA, Yin H, Chang NC, Wilson DH, Frenette J, Rudnicki MA. 2014. Inhibition of JAK-STAT signaling stimulates adult satellite cell function. *Nat Med.* **20**:1174–1181.

Prins GS, Huang L, Birch L, Pu Y. 2006. The role of estrogens in normal and abnormal development of the prostate gland. *Ann N Y Acad Sci.* **1089**:1–13.

Prüfer K. 2018. snpAD: an ancient DNA genotype caller. *Bioinformatics* **34**:4165–4171.

Raghavan M, Skoglund P, Graf KE, Metspalu M, Albrechtsen A, Moltke I, Rasmussen S, Stafford TW Jr, Orlando L, Metspalu E, et al. 2014. Upper Palaeolithic Siberian genome reveals dual ancestry of Native Americans. *Nature* **505**:87–91.

Reich D, Thangaraj K, Patterson N, Price AL, Singh L. 2009. Reconstructing Indian population history. *Nature* **461**:489–494.

Rettberg JR, Yao J, Brinton RD. 2014. Estrogen: a master regulator of bioenergetic systems in the brain and body. *Front Neuroendocrinol.* **35**:8–30.

Rimbault M, Beale HC, Schoenebeck JJ, Hoopes BC, Allen JJ, Kilroy-Glynn P, Wayne RK, Sutter NB, Ostrander EA. 2013. Derived variants at six genes explain nearly half of size reduction in dog breeds. *Genome Res.* **23**:1985–1995.

Robinson DR, Wu YM, Vats P, Su F, Lonigro RJ, Cao X, Kalyana-Sundaram S, Wang R, Ning Y, Hodges L, et al. 2013. Activating ESR1 mutations in hormone-resistant metastatic breast cancer. *Nat Genet.* **45**:1446–1451.

Rose RJ, Bloomberg MS. 1989. Responses to sprint exercise in the greyhound: effects on haematology, serum biochemistry and muscle metabolites. *Res Vet Sci.* **47**:212–218.

Rose AJ, Kiens B, Richter EA. 2006. Ca^{2+}-calmodulin-dependent protein kinase expression and signalling in skeletal muscle during exercise. *Journal of physiology.* **574**:889–903.

Rueness EK, Asmyhr MG, Sillero-Zubiri C, Macdonald DW, Bekele A, Atickem A, Stenseth NC. 2011. The cryptic African wolf: *Canis aureus* lupaster is not a golden jackal and is not endemic to Egypt. *PLoS One* **6**:e16385.

Sabeti PC, Varilly P, Fry B, Lohmueller J, Hostetter E, Cotsapas C, Xie X, Byrne EH, McCarroll SA, Gaudet R, et al. 2007. Genome-wide detection and characterization of positive selection in human populations. *Nature* **449**:913–918.

Savolainen P, Zhang YP, Luo J, Lundeberg J, Leitner T. 2002. Genetic evidence for an East Asian origin of domestic dogs. *Science* **298**: 1610–1613.

Schmutz SM, Berryere TG, Goldfinch AD. 2002. TYRP1 and MC1R genotypes and their effects on coat color in dogs. *Mamm Genome.* **13**:380–387.

Scruggs SB, Wang D, Ping P. 2016. PRKCE gene encoding protein kinase C-epsilon—dual roles at sarcomeres and mitochondria in cardiomyocytes. *Gene* **590**:90–96.

Shan S, Xu F, Brenig B. 2021. Genome-wide association studies reveal neurological genes for dog herding, predation, temperament, and trainability traits. *Front Vet Sci.* **8**:693290.

Sims NA, Clement-Lacroix P, Minet D, Fraslon-Vanhulle C, Gaillard-Kelly M, Resche-Rigon M, Baron R. 2003. A functional androgen receptor is not sufficient to allow estradiol to protect bone after gonadectomy in estradiol receptor-deficient mice. *J Clin Invest.* **111**:1319–1327.

Sutter NB, Ostrander EA. 2004. Dog star rising: the canine genetic system. *Nat Rev Genet.* **5**:900–910.

Szpiech ZA, Hernandez RD. 2014. selscan: an efficient multithreaded program to perform EHH-based scans for positive selection. *Mol Biol Evol.* **31**:2824–2827.

Tamura K, Dudley J, Nei M, Kumar S. 2007. MEGA4: Molecular Evolutionary Genetics Analysis (MEGA) software version 4.0. *Mol Biol Evol.* **24**:1596–1599.

Tchernof A, Poehlman ET, Després JP. 2000. Body fat distribution, the menopause transition, and hormone replacement therapy. *Diabetes Metab.* **26**:12–20.

Thalmann O, Shapiro B, Cui P, Schuenemann VJ, Sawyer SK, Greenfield DL, Germonpre MB, Sablin MV, Lopez-Giraldez F, Domingo-Roura X, et al. 2013. Complete mitochondrial genomes of ancient canids suggest a European origin of domestic dogs. *Science* **342**:871–874.

Viranta S, Atickem A, Werdelin L, Stenseth NC. 2017. Rediscovering a forgotten canid species. *BMC Zoology* **2**:6.

Voillet V, San Cristobal M, Pere MC, Billon Y, Canario L, Liaubet L, Lefaucheur L. 2018. Integrated analysis of proteomic and transcriptomic data highlights late fetal muscle maturation process. *Mol Cell Proteomics.* **17**:672–693.

Wang K, Li M, Hakonarson H. 2010. Analysing biological pathways in genome-wide association studies. *Nat Rev Genet.* **11**: 843–854.

Wang GD, Zhai W, Yang HC, Wang L, Zhong L, Liu YH, Fan RX, Yin TT, Zhu CL, Poyarkov AD, et al. 2016. Out of southern East Asia: the natural history of domestic dogs across the world. *Cell Res.* **26**:21–33.

Wayne RK, Ostrander EA. 1999. Origin, genetic diversity, and genome structure of the domestic dog. *Bioessays* **21**:247–257.

Weise M, De-Levi S, Barnes KM, Gafni RI, Abad V, Baron J. 2001. Effects of estrogen on growth plate senescence and epiphyseal fusion. *Proc Natl Acad Sci U S A.* **98**:6871–6876.

Yang Q, Chen H, Ye J, Liu C, Wei R, Chen C, Huang L. 2019. Genetic diversity and signatures of selection in 15 Chinese indigenous dog breeds revealed by genome-wide SNPs. *Front Genet.* **10**:1174.

Yang J, Lee SH, Goddard ME, Visscher PM. 2011. GCTA: a tool for Genome-wide Complex Trait Analysis. *Am J Hum Genet.* **88**:76–82.

Zaldivar-Lopez S, Marin LM, Iazbik MC, Westendorf-Stingle N, Hensley S, Couto CG. 2011. Clinical pathology of Greyhounds and other sighthounds. *Vet Clin Pathol.* **40**:414–425.

Zeng F, Zhou L, Tang Z. 2016. A study for association and interaction analysis to metabolic syndrome and the ESR1 gene on cardiovascular autonomic neuropathy in a Chinese Han population. *Diabetol Metab Syndr.* **8**:42.

Zhang L, Wang Y, Wu G, Rao L, Wei Y, Yue H, Yuan T, Yang P, Xiong F, Zhang S, *et al.* 2020. Blockade of JAK2 protects mice against hypoxia-induced pulmonary arterial hypertension by repressing pulmonary arterial smooth muscle cell proliferation. *Cell Prolif.* **53**:e12742.

Zhang T, Maier LS, Dalton ND, Miyamoto S, Ross J Jr, Bers DM, Brown JH. 2003. The δ_C isoform of CaMKII is activated in cardiac hypertrophy and induces dilated cardiomyopathy and heart failure. *Circ Res.* **92**:912–919.

Zhou QJ, Liu X, Zhang L, Wang R, Yin T, Li X, Li G, He Y, Ding Z, Ma P, *et al.* 2022. A single-nucleus transcriptomic atlas of the dog hippocampus reveals the potential relationship between specific cell types and domestication. *Natl Sci Rev.* **9**:nwac147.

Zhou Y, Zhou B, Pache L, Chang M, Khodabakhshi AH, Tanaseichuk O, Benner C, Chanda SK. 2019. Metascape provides a biologist-oriented resource for the analysis of systems-level datasets. *Nat Commun.* **10**:1523.